Determination of Modal Constant for Fundamental Frequency of Perforated Plate by Rayleigh's Method using Experimental Values of Natural Frequency

Kiran D. Mali and Pravin M. Singru

Department of Mechanical Engineering, Birla Institute of Technology and Science, Pilani, K.K. Birla Goa Campus, NH-17B, Zuarinagar, Goa, India- 403726

In the present work, an expression for the modal constant of the fundamental frequency of the perforated plate was determined experimentally. Rayleigh's formulation was used to calculate the modal constant. The displacement solution was considered to be a linear combination of cosines. In Rayleigh's formulation, fundamental frequency values were taken from experimental analysis. This problem was solved in reverse order by considering known experimental values of the fundamental frequency. Thus, the modal constant expression for fundamental frequency was discovered.

NOMENCLATURE

A	Correction factor
AR	Aspect ratio = $L_y/Lx, = b/a$
L_h	Centre to centre distance between holes along width in mm
L_v	Centre to centre distance between holes along length in mm
$(d + h_r)$	Center to center distance in mm
	Density of material in kg/m³
D	Diameter of perforation hole in mm
a	Dimension of plate along X axis
b	Dimension of plate along Y axis
L_x	Effective plate width in mm
E	Young's modulus in N/m²,
L_Y	Effective plate length in mm
h	Effective plate thickness in mm
T, u	Kinetic and strain energy of the plate respectively
h_r	Ligament width in mm
η_l	Ligament efficiency
MRR	Mass remnant ratio
ω_1	Fundamental frequency of perforated plate in Hz
v	Poisson's ratio
r	Radius of perforation hole in mm
λ	Modal constant
D	Flexural rigidity of the plate = $Eh^3/12(1 - v^2)$

1. INTRODUCTION

Cutouts are found in mechanical, civil, marine and aerospace structures, commonly as access ports for mechanical and electrical systems or simply to reduce weight. Cutouts are also made to provide ventilation and to modify the resonant frequency of the structures. Perforated plates are often utilized as head plates, end covers, or supports for tube bundles, typically including tube sheets and support plates. Perforated plates are widely used in nuclear power equipment, heat exchangers, and pressure vessels. The holes in the plate are arranged in various regular penetration patterns. Industrial applications include both square and triangular array perforation patterns.

Many researchers have carried out studies of perforated plate structures. Monahan et al. studied the finite element analysis of a clamped plate with different cutout sizes along with experiments using holographic interferometry.[1] Paramsivam used a finite difference approach in analyzing the effects of openings on the fundamental frequencies of plates with simply supported and clamped boundary conditions.[2] O'Donnell determined the effective elastic constants for thin perforated plates by equating the strains in an equivalent solid material to the average strains in the perforated material.[3] Hegarty and Ariman investigated free vibrations of rectangular elastic plate either clamped or simply supported with a central circular hole using the least-squares point-matching method.[4] Aksu and Ali obtained dynamic characteristics of rectangular plates with one or two cutouts using a finite difference formulation along with experimental verifications.[5] Ali and Atwal studied the natural frequencies of simply supported rectangular plates and rectangular cutouts using the Raleigh Ritz method.[6] Reddy studied linear and large amplitude flexural vibration of isotropic and composite plates with cutout by using the finite element method.[7] Chang and Chiang studied the vibration of a rectangular plate with an interior cutout by using the finite element method.[8] Lam et al. presented an efficient and accurate numerical method in the study of the vibration of rectangular plates with cutouts and non- homogeneity.[9] They found the deflection function for the originally complex domain by dividing the problem domain into appropriate rectangular segments. Lam and Hung investigatedflexural vibrations of plates with discontinuities in the form of cracks and cutouts using a scheme that combines the flexibility of dividing the problem domain into appropriate segments and the high accuracy resulting from the use of orthogonal polynomial functions, generated using the Gram-Schmidt process.[10] Lee et al. predicted the natural frequencies of rectangular plates with an arbitrarily located rectangular cutout.[11] Mundkur et al. studied the vibration of square plates with square cutouts by using boundary characteristics orthogonal polynomials satisfying the bound-

ary conditions.[12] Burgemeister and Hansen showed that effective material constants could not be used in classical equations to accurately predict the resonance frequencies of simply supported perforated panels.[13] Instead, it is much more accurate to fit the results from ANSYS to a simple cubic function. This function can be used to determine the effective resonance frequency ratio for a large range of panel geometries with an error of less than 3%. Young et al. studied the free vibration of thick rectangular plates with depression, grooves, or cutouts using three-dimensional elasticity and Ritz method.[14] Sivasubramonian et al. investigated the free vibration characteristics of unstiffened and longitudinally stiffened square panels with symmetrical square cutouts by using the finite element method.[15, 16] The optimized Rayleigh-Ritz method was applied by Grossi et al. to generate values of the fundamental frequency coefficient and the one corresponding to the first fully antisymmetric mode for rectangular plates elastically restrained against rotation and with located circular holes.[17] Suhn et al. performed a finite element modal analysis of the perforated plates having square and triangular hole patterns.[18] They carried out a modal analysis of the plates by using existing equivalent elastic properties. They also verified feasibility of the finite element models by conducting a modal test on one typical perforated plate. Parameters, such as natural frequencies and mode shapes, were extracted and compared with the analysis results. Huang and Sakiyama analyzed the free vibration of rectangular plates with variously shaped holes.[19] Sahu and Datta studied the parametric instability behavior of curved panels with cutouts subjected to in-plane static and periodic compressive edge loadings using the finite element analysis.[20] The first order shear deformation theory was used to model the curved panels, considering the effects of transverse shear deformation and rotary inertia. Avalos and Laura performed a series of numerical experiments on vibrating simply supported rectangular plates with two rectangular holes with free edges.[21] Liew et al. presented an analysis of free vibration of plates with internal discontinuities due to central cut-outs.[22] A numerical formulation for the basic L-shaped element, which was divided in to appropriate subdomains that were dependent upon the location of the cut out was used as the basic building element. Wang and Lai adopted the hybrid method, which combined experimental and numerical methods, to investigate the dynamic behavior of perforated plates.[23] The equivalent material properties of the perforated plates were also obtained by the hybrid method. In addition, the curve-fitting technique was utilized to find the relationship of the mass remnant ratio with the parameter ratio. They obtained functions from the curve fitting and used them to accurately predict the equivalent material properties and resonant frequencies of perforated plates of the diagonal array. Sinha et al. suggested a formula for added mass of the vibrating perforated plate-type structures submerged in fluid based on experimental and analytical studies on a number of test specimens.[24] Wu et al. developed a mathematical model of axisymmetric elastic/plastic perforated circular plates for bending and stretching.[25] Bhattacharya and Raj analyzed a quarter symmetric part of a perforated plate containing a 3×3 square array of circular holes by the finite element method (FEM) to obtain the peak stress multipliers under membrane and bending loads for different biaxiality ratios.[26] Britan et al. experimentally and theoretically/numerically studied the flow and wave pattern that resulted from the interaction of an incident shock wave with a few different types of barriers, all having the same porosity but different geometries.[27] Bhattacharya, and Raj also developed second- and fourth- order polynomials describing

the yield criterion for perforated plates with square penetration patterns.[28] They did not consider the effect of out-of-plane stresses in the investigation, as these are found to be negligible in the case of thin perforated plates, for which plane stress condition was assumed in the finite element. Pedersen studied the optimization of the hole of a given area, which is placed in the interior of a plate with an arbitrary external boundary.[29] The objectives of the optimization were the eigenfrequencies of the plate with the hole. The optimization was performed in relation to maximizing the first eigenfrequency or maximizing the gap between the first and second eigenfrequency. Lee and Kim studied the validity of the Eshelby-type model for predicting the effective Young's modulus and in-plane Poisson's ratio of two dimensional perforated plates in terms of porosity size and arrangement.[30] Azhari et al. established the nonlinear mathematical theory for initial- and post-local buckling analysis of plates of abruptly varying stiffness based on the principle of virtual work.[31] They programmed the method, and several numerical examples were presented to demonstrate the scope and efficacy of the procedure. Local buckling coefficients of perforated and stepped plates were obtained, and the results were compared with known solutions. They studied the postbuckling behaviour of perforated and stepped plates for different geometries. Rezaeepazhand and Jafari used analytical investigation to study the stress analysis of plates with different central cutouts.[32] Particular emphasis was placed on flat square plates subjected to a uni-axial tension load. They compared results based on analytical solution with the results obtained using finite element methods. Hung and Jo studied free vibration characteristics of a circular perforated plate submerged in fluid with rectangular and square penetration patterns.[33] The natural frequencies were obtained by theoretical calculations and three-dimensional finite element analyses. The effect of holes on the modal characteristics was investigated; they also proposed new equivalent elastic constants for the modal analysis of a perforated plate. Watanabe and Koike investigated fatigue strength and creep-fatigue strength of perforated plates having stress concentration.[34] The specimens were made of type 304 SUS stainless steel, and the temperature was kept to 550°C. The entirety of each cycle of the experiment record was analyzed, and the characteristics of the structures having stress concentration were discussed. They also studied the stress redistribution locus in evaluation plastic behavior in a cyclic fatigue process as well as a stress relaxation in creep process, and the feasibility was discussed in conjunction with the comparison to experimental results. Jeong and Amabili presented a theoretical study on the natural frequencies and the mode shapes of perforated beams in contact with an ideal liquid.[35] The work of Kathagea et al. deals with the design of perforated trapezoidal sheeting.[36] They calculated the effective stiffness values for perforated sheeting with different arrays of holes based on numerical analyses and graphs. Also given was the calculation of a buckling coefficient for a perforated plate under uniform in-plane compression loading and the calculation for an infinitely long perforated plate under shear loading. Paik studied the ultimate strength characteristics of perforated steel plates under edge shear loading[37] and under combined biaxial compression and edge shear loads.[38] Liu et al. studied the effect of the cracks on natural frequencies and the modal strain energy of a perforated plate with ligament fractured cracks by finite element analysis.[39] Cheng and Zhao studied buckling behaviors of uni-axially compressed perforated steel plates strengthened by four types of stiffeners: ringed stiffener, flat stiffener, longitudinal stiffener, and transverse stiffener.[40]

Romero et al. used digital speckle interferometry technique for tuning resonant frequencies of vibrating plates in order to investigate the dynamical behavior of perforated plates.[41] Experimental natural frequencies and modal shapes were compared to those obtained by an analytical approximate solution based on the Rayleigh–Ritz method with the use of orthogonal polynomials as coordinate functions. Mali and Singru introduced the concept of concentrated negative masses for perforation holes and determined the fundamental frequency of a rectangular plate carrying four circular perforations in a rectangular pattern.[42,43] Mali and Singru formulated analytical models by using the greatest integer functions and unit step functions to express non-homogeneity in Young's modulus and the density and determined fundamental frequency of free vibration of a perforated plate.[44–46]

Many studies have been done on perforated plates having rectangular/square and triangular arrays of holes, especially in regards static behavior and stress distribution in the plate. Present literature on the dynamic performance of perforated plates deals with equivalent properties of material. These equivalent material properties can be used to consider perforated plates as full solid plates in vibration analysis. The effect of the hole geometry, hole size, ligament efficiency, and plate support conditions on the dynamic behavior of rectangular plates has not been experimentally studied thus far in combination and or by using FEM. There is no evidence of the formulation of modal constants, functions from curve fitting, or empirical equations to accurately predict the effective resonance frequencies of a wide range of perforation geometries, for rectangular plates with rectangular penetration pattern, or for all edges with clamped support condition.

In the present study, Rayleigh's formulation for perforated plates is carried out by considering a perforated rectangular plate as a full solid plate. Rayleigh's formulation gives an expression for fundamental frequency in terms of equivalent outer dimensions of solid plates and material properties.

Further, Rayleigh's formulation for fundamental frequency is modified with the known value of a fundamental frequency obtained from experimental analysis and by considering actual geometrical parameters of the perforated plate. This modified expression is rearranged to produce an expression for a modal constant.

The proposed approach provides an alternative method to the existing equivalent material properties approach. This modal constant can be directly used to calculate fundamental frequency by using actual material properties instead of equivalent material properties.

In this work, the perforation pattern considered is rectangular with circular perforations. The boundary condition considered is clamped-clamped. Thus, the proposed approach permits the ready determination of reasonably accurate natural frequencies for a plate involving any combination of ligament efficiency and perforation diameter. Presented are the finite element method (FEM) analysis and experimental analysis results for two plates within a given test envelope and outside a test envelope in order to illustrate the applicability and accuracy of the approach.

2. ANALYTICAL FORMULATION

The fundamental frequency expression of a plate is formulated by Rayleigh's principle.[47] This formulation is carried out by considering the perforated plate as a solid plate with the same outer dimensions as that of a perforated plate. Rayleigh's principle is based on the statement, 'If the vibrating system is conservative (no energy is added or lost), then the maximum kinetic energy, T_{max}, must be equal to the maximum potential (strain) energy, u_{max}'. In order to apply this principle, the elastic plate undergoing free vibrations in fundamental mode is considered as a system with one degree of freedom. Kinetic Energy of plate T is given as,

$$T = \frac{1}{2} \iint\limits_R h\rho\, \dot{w}^2(x,y,t) dx dy\,. \tag{1}$$

Assuming that the plate is undergoing harmonic vibrations, then the vibrating middle surface of the plate can be approximated by the equation

$$w(x,y,t) = W_1(x,y)\cos\omega_1 t; \tag{2}$$

where $W_1(x,y)$ is a continuous function that approximately represents the shape of the plate's deflected middle surface and satisfies at least the kinematic boundary conditions, and ω_1 represents the natural frequency of the plate pertinent to the assumed shape function. Assume $\omega = \omega_1$ would be its fundamental frequency.

The maximum value of Kinetic Energy is obtained at

$$\sin^2\omega_1 t = 1; \tag{3}$$

$$T_{\max} = \frac{\omega^2_1}{2}\sin^2\omega_1 t \iint\limits_R h\rho\, \dot{W}^2_1(x,y,) dx dy$$
$$= \frac{1}{2}\omega_1{}^2 \iint\limits_R h\rho\, \dot{W}^2_1(x,y,) dx dy\,. \tag{4}$$

Maximum Strain Energy is given as,

$$u_{\max} = \frac{1}{2} \iint\limits_R D[(\nabla^2 W_1)^2 + 2(1-v)\{(\frac{\partial^2 W_1}{\partial x \partial y})^2$$
$$- \frac{\partial^2 W_1}{\partial x}\frac{\partial^2 W_1}{\partial y}\}] dx dy. \tag{5}$$

For conservative system by Rayleigh's principal,

$$T_{\max} = u_{\max}. \tag{6}$$

From equation (4) and (5), we obtain (7)

$$W_{1,xy} = \frac{\partial^2 W_1}{\partial x \partial y} \quad W_{1,xx} = \frac{\partial^2 W_1}{\partial x^2} \quad W_{1,yy} = \frac{\partial^2 W_1}{\partial y^2}; \tag{8}$$

Equation (7) is called Rayleigh's Quotient and gives the fundamental natural frequency of the plate.

For constant thickness and homogeneous plates, D, ρ, and h are constant. Hence, Rayleigh's Quotient becomes, (9) From Eq. (2) and for the orientation of the plate shown in Fig. 1, assuming the solution of the form,

$$W_1(x,y) = \left[1 + \cos\frac{\pi x}{a}\right]\left[1 + \cos\frac{\pi y}{b}\right]$$
$$\text{where} \quad \begin{cases} 0 \leqslant x \leqslant a \\ 0 \leqslant y \leqslant b \end{cases}. \tag{10}$$

$$\omega^2{}_1 = \frac{\iint\limits_{R} D[(\nabla^2 W_1)^2 + 2(1-\upsilon)\{W^2{}_{1,xy} - W_{1,xx}W_{1,yy}\}]dxdy}{h\rho \iint\limits_{R} W_1{}^2 dxdy}; \qquad (7)$$

$$\omega^2{}_1 = \frac{D\int\limits_{0}^{a}\int\limits_{0}^{b} [(\nabla^2 W_1)^2 + 2(1-\upsilon)\{W^2{}_{1,xy} - W_{1,xx}W_{1,yy}\}]dxdy}{h\rho \int\limits_{0}^{a}\int\limits_{0}^{b} W_1{}^2 dxdy}; \qquad (9)$$
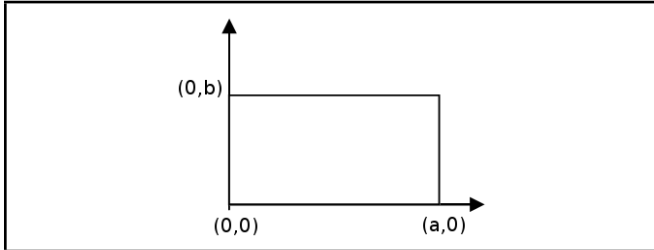
Figure 1. Co-ordinates of the plate.

3. ANALYTICAL SOLUTION

Fundamental frequency ω_1, is obtained by substituting Eq. (10) in Eq. (9) as follows:

$$\omega_1{}^2 = \frac{9D\pi^4}{h\rho a^4 b^4}\left[3\left(a^2 b^2\right)b^2 + \left(a^2 b^2\right)a^2 + 2a^2 b^2 \right.$$
$$\left. + 2a^2 b^2(1-\upsilon^2)\right]. \qquad (11)$$

This fundamental frequency equation is further modified by including perforation parameters given by Eq. (18) to get the fundamental frequency Eq. (21) for the perforated plate.

The expression given by Eq. (11) is used to calculate values of the correction factor (A), from known natural frequencies, obtained by experimental analysis.

4. GEOMETRY OF PERFORATED PLATE WITH RECTANGULAR PERFORATION PATTERN

From Fig. 2 consider the triangle ABC with area J as

$$J = \frac{L_h L_v}{2} - \left[\frac{\pi r^2}{4} + \frac{\pi r^2}{4}\right] = \frac{L_h L_v}{2} - \left[\frac{2\pi r^2}{4}\right]; \quad (12)$$

and the number of triangular elements N as

$$N = 2\left[\frac{L_x}{L_h}\frac{L_y}{L_v}\right]. \qquad (13)$$

The total area of the perforated plate is $K = J \times N$, where

$$K = L_x L_y - \frac{L_x L_y \pi r^2}{L_h L_v}. \qquad (14)$$

The mass remnant ratio (MRR) is defined as the ratio of the perforated plate area to the area of the full solid plate of the same outer dimensions. It can be expressed as

$$MRR = \frac{K}{L_x L_y}; \qquad (15)$$

where $(L_x L_y)$ is the area of the full solid plate

$$MRR = 1 - \frac{\pi r^2}{L_h L_v}; \qquad (16)$$
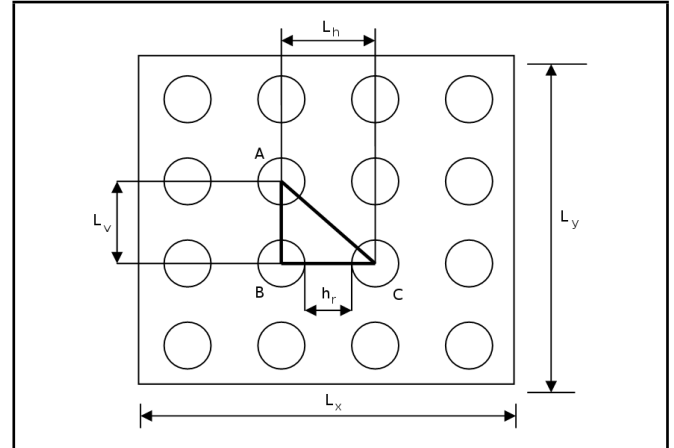
Figure 2. Geometry of the perforated plate.

Table 1. Details of the specimens analyzed experimentally.

η_l	Pitch $(d + h_r)$, (mm)	h_r, (mm)	MRR
For $d = 6$ mm hole			
0.2	7.5	1.5	0.4973
0.6	15	9	0.874
For $d = 9$ mm hole			
0.4	15	6	0.7172
For $d = 12$ mm hole			
0.6	30	18	0.8743

$$MRR = \frac{ab}{ab} - \frac{ab\pi r^2}{ab L_h L_v} = 1 - \frac{ab\pi r^2}{ab L_h L_v}. \qquad (17)$$

Thus, the relation between perforation parameters MRR, L_h, L_v, r and plate dimensions a, b is

$$ab = \frac{(1 - MRR) L_h L_v ab}{\pi r^2}. \qquad (18)$$

The relation between the ligament efficiency, pitch, and ligament width is

$$\eta_l = \frac{(h_r)}{(d + h_r)}; \qquad (19)$$

for case the under study

$$L_h = L_v = (d + h_r). \qquad (20)$$

5. MATERIALS AND METHOD

Fundamental frequency is obtained experimentally, for four specimens with configurations shown in Table 1. All the specimens are analyzed for the boundary condition clamped on all four edges. The correction factor is determined from Eq. (22) for each specimen from the average values of the fundamental frequencies obtained experimentally.[48]
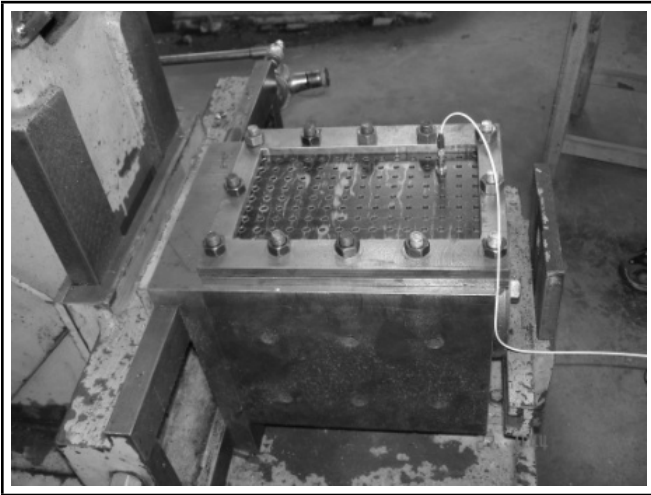
Figure 4. The fixture and specimen.
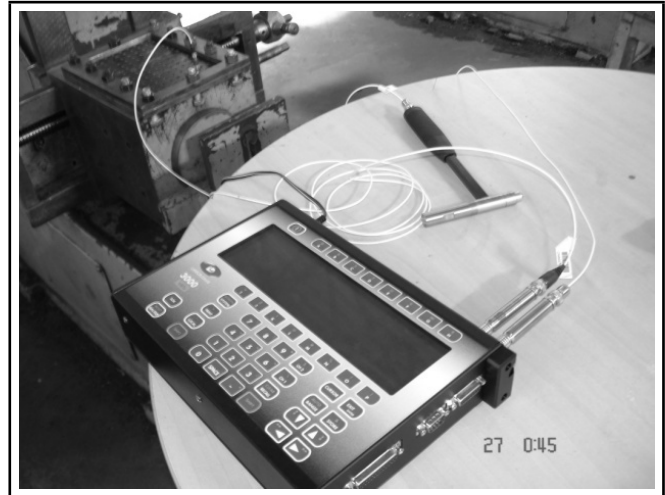
Figure 5. Experimental set up.

5.1. Experimental Analysis

This section covers the information about the test specimen, clamping details, and experimental set-up used in the experimental vibration analysis.[48,49] Specimens were prepared for ligament efficiency 0.2, 0.4 and 0.6 and perforation diameters 6 mm, 9 mm, and 12 mm. Each specimen was tested ten times, and the average value of fundamental frequency was obtained. The outer dimensions of all the specimens were 259 mm by 207 mm by 2 mm, but effective dimensions of the perforated area were 216 mm by 138 mm. All specimens were made of mild steel material with an aspect ratio $b/a = 1.565$. The following is the material properties considered for all specimens: $E = 2.1 \times 10^{11} \text{N/m}^2$, $v = 0.3$, $\rho = 7850 \text{ kg/m}^3$

5.2. Test Specimen and Test Fixture

Figure 3 shows the schematic of the specimens used for testing and fixture plate. The margin with holes (outside the effective area) were kept to clamp the specimens between two fixture plates to get the clamed-clamped boundary condition on all four edges of the specimen. The test fixture mainly consisted of two rectangular plates of outer dimensions 259 mm by 207 mm by 9.2 mm. Both these fixture plates had central rectangular cut-outs with dimensions of 216 mm by 138 mm, which were aligned concentrically one over the other. The test specimen with all four outside edges fixed was held centrally between these fixture plates.

Figure 3 shows one of two similar fixture plates with central rectangular cut-outs and holes along the circumference for bolting the plates firmly. These fixture plates, with the test specimen sandwiched, were clamped together by using nut-bolt assembly in the holes provided along the circumference of fixture plates as shown in Figure 4. Thus, the required boundary condition of all four outside edges fixed was achieved.

5.3. Experimental Set up and Procedure

Experimentation was conduced by means of two channel FFT (Model: Virte 300+, Larson and Davis inc, U.S.A.) analyzers, an impact hammer (Model: 086C03, PCB Piezotronics Inc., U.S.A.), and an accelerometer (Model: 352C68, PCB Piezotronics Inc., U.S.A.).[47,48] Figure 5 shows the experimental set up used for testing, and Figure 6 shows schematic of the experimental set up. Care was taken in applying uniform pressure at all bolts with the help of a torque wrench. Four sam-
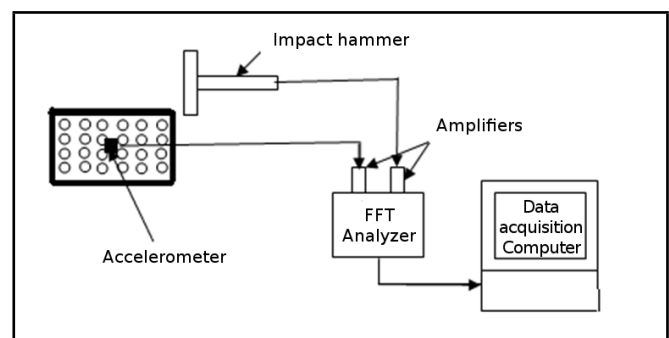
Figure 6. Schematic of experimental set-up.

pling points were chosen for mounting the accelerometer from the driving point survey such that the node would not occur at these points. A fixed response method was used for taking readings. The transfer function of each sampling point was calculated by the spectrum analyzer and was recorded at sixteen impacts to get the final spectrum for each specimen plate. Such experiments were repeated ten times. The final results of the natural frequencies for each specimen plate were mean values of the ten readings. The final values of natural frequency were tabulated in the last column of the Table 2. The dynamic mass of the accelerometer was much less than that of the plate, so the influence of the mass of the accelerometer on the dynamic behavior of the specimen could be neglected.

6. RESULTS AND DISCUSSION

The average value of the fundamental frequency of each specimen from Table 2 was used to calculate the value of the correction factor for respective specimens.

6.1. Determination of the Modal Constant

The expression for the natural frequency of the solid plate given by Eq. (11) could be modified by considering actual geometrical parameters of the perforated plate. Geometrical parameters of the perforated plate were related to the full solid plate dimensions by the relation given in Eq. (18). The expression in Eq. (21) can not be used directly to calculate the fundamental frequency of the perforated plate unless the correction factor is considered.

After simplification and after considering the correction fac-
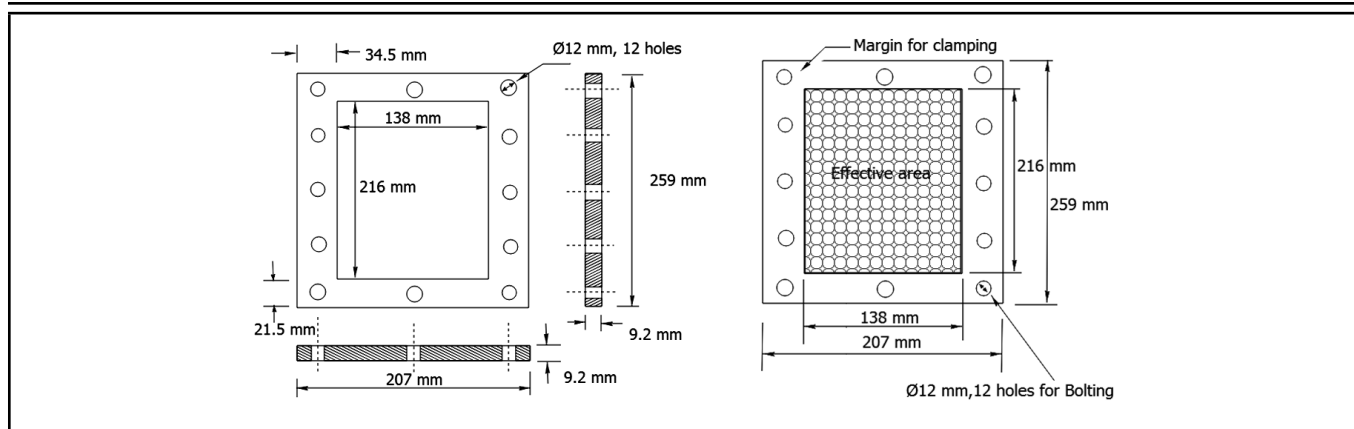
Figure 3. Schematic of the fixture plate and specimens used for experimentation.

Table 2. Experimentally obtained values of fundamental frequency.

η_1	Pitch d, (mm)	Fundamental frequency,(No. of Runs) Hz										
		1	2	3	4	5	6	7	8	9	10	Avg.
0.2	6	602	596	596	599	599	580	583	583	586	583	590.7
0.6	6	615	615	618	615	618	615	615	621	615	615	616.2
0.4	9	571	571	571	571	571	571	571	571	571	571	571
0.6	12	586	586	586	586	586	586	590	590	590	590	587.6

$$\omega_1{}^2 = \frac{9D\pi^4}{h\rho \left[\frac{(1-MRR)L_hL_vab}{\pi r^2}\right]^4} \left[\begin{array}{l} 3\left[\frac{(1-MRR)L_hL_vab}{\pi r^2}\right]^2 b^2 + \left[\frac{(1-MRR)L_hL_vab}{\pi r^2}\right]^2 a^2 + \\ 2\left[\frac{(1-MRR)L_hL_vab}{\pi r^2}\right]^2 + 2\left[\frac{(1-MRR)L_hL_vab}{\pi r^2}\right]^2 (1-v^2) \end{array} \right]; \qquad (21)$$

tor, Eq. (21) becomes

$$\omega_1{}^2 = \frac{9D\pi^6 r^4}{h\rho[(1-MRR)L_hL_vab]^2} \cdot$$
$$\cdot \left[3b^2 + a^2 + 2 + 2(1-v^2)\right] (A); \qquad (22)$$

where A is introduced as the correction factor. Values of the correction factor are calculated from Eq. (22) by using fundamental frequencies determined experimentally, tabulated in the last column of Table 2. Correction factor values are tabulated in Table 3 for different specimens. Equation 22 can be used for calculating the fundamental frequency of the perforated plate by substituting the average value of correction factor 'A', from Table 3. A simple approximate formula for the fundamental natural frequency of the flexural vibration of the rectangular isotropic perforated plate is given as,[50]

$$\omega_1 \approx \sqrt{\frac{\lambda D}{h\rho}}; \qquad (23)$$

where λ is the modal constant.

Thus, the modal constant λ for fundamental frequency is obtained from Eqs. (22) & (23).

$$\lambda = \left[\frac{9\pi^6 r^4}{[(1-MRR)L_hL_vab]^2} \cdot \right.$$
$$\left. \cdot \left[3b^2 + a^2 + 2 + 2(1-v^2)\right](A)\right]; \qquad (24)$$

$$\lambda = \left[\frac{9\pi^6 r^4}{[(1-MRR)L_hL_vab]^2} \cdot \right.$$
$$\left. \cdot \left[3b^2 + a^2 + 2 + 2(1-v^2)\right](0.009129)\right]. \qquad (25)$$

The expression given by Eq. (24) can be used to calculate the modal constant λ for the fundamental natural frequency of the perforated plates with rectangular perforation patterns of circular perforations having different configurations.

6.2. Application and Accuracy of the Approach

The proposed approach is validated by additional experimental analysis and by running FEM simulations with AN-SYS. Configurations of the specimens are given in Tables 4 & Table 5. The criteria followed to select the plate dimensions in the analysis were

1. Validating the results of the proposed approach within the test envelope, or the effective outer dimensions (a, b) that were the same as the specimens given in Section 5.

2. Validating the results of the proposed approach outside the test envelope, or the effective outer dimensions (a, b) that were different from the specimens given in Section 5.

FEM analysis was carried out by using the shell63 element. It is assumed that the structure is formed from isotropic homogeneous elastic material, or mild steel. Effective outside dimensions, thickness, and material properties of the first specimen analyzed are the same as that used in the test envelope and within the fixture limit, but configuration is different from the test envelope. However, the second specimen thickness and material properties were the same as that used in the test envelope, but the effective outside dimensions (a, b) and configurations were different from the test envelope. Due to the size limitations of the test fixture experimental validation was not carried out for second case as given in Table 5. It was found that the results obtained from the proposed method are in close

Table 3. Values of the correction factor for different specimens

Sr. no.	η_l	d, mm	MRR	L_h, mm	L_v, mm	ω_{1avg}	Value of A
1	0.2	6	0.4973	7.5	7.5	590.7	0.009099
2	0.6	6	0.8743	15	15	616.2	0.009906
3	0.4	9	0.7172	15	15	571	0.008504
4	0.6	12	0.8743	30	30	587.6	0.009007
						Average Value of 'A' =	0.009129

Table 4. Validation of the modal constant within the test envelope.

a, mm	b, mm	d, mm	η_l	$L_h = L_v$, mm	MRR	ω_1 With modal Constant, Hz	ω_1, ANSYS, Hz	ω_1 With Experimental Analysis, Hz
138	216	9	0.4	15	0.7172	591.60	612.62	571

Table 5. Validation of the modal constant outside the test envelope.

a, mm	b, mm	d, mm	η_l	$L_h = L_v$, mm	MRR	ω_1 With modal Constant, Hz	ω_1, ANSYS, Hz
550	860	50	0.6	125	0.87433	47.07	42

agreement with the experimental and FEM results within test envelope and are in close agreement with the FEM results outside the test envelope.

7. CONCLUSION

In the present work, the expression for the modal constant for fundamental frequency of the perforated plate was determined. To establish this modal constant, experimental vibration data was used. A simple approximate formula for the fundamental natural frequency of flexural vibration of a rectangular isotropic perforated plate was developed. Rayleigh's method was used in combination with experimental values of the natural frequency to establish the expression for the modal constant. The fundamental frequency calculated by using this modal constant is in good agreement with ANSYS result. Thus, this approach provides an alternative method to the equivalent elastic properties method of the perforated plate for finding natural frequency.

REFERENCES

[1] Monahan, J., Nemergut, P. J., and Maddux, G. E. Natural frequencies and mode shapes of plates with interior cutouts, *The Shock and Vibration Bulletin*, **41**(7), 37–49, (1970).

[2] Paramsivam, P. Free vibration of square plates with square openings, *Journal of Sound and Vibration*, **30**(2), 173–178, (1973).

[3] O'Donnell, W. J. Effective elastic constants for the bending of thin perforated plates with triangular and square penetration patterns, *Journal of Engineering for Industry*, **95**(1), 121–128, (1973).

[4] Hegarty, R. F. and Ariman, T. Elasto-dynamic analysis of rectangular plates with circular holes, *International Journal of Solids Structures*, **11**(7–8), 895–906, (1975).

[5] Aksu, G. and Ali, R. Determination of dynamic characteristics of rectangular plates with cutouts using a finite difference formulation, *Journal of Sound and Vibration*, **44**(1), 147–158, (1976).

[6] Ali, R. and Atwal, S. J. Prediction of natural frequencies of vibration of rectangular plates with rectangular cutouts, *Computers and Structures*, **12**(6), 819–823, (1980).

[7] Reddy, J. N. Large amplitude flexural vibration of layered composite plates with cutout, *Journal of Sound and Vibration*, **83**(1), 1–10, (1982).

[8] Chang, C. N. and Chiang, F. K. Vibration analysis of a thick plate with an interior cutout by a finite element method, *Journal of Sound and Vibration*, **125**(3), 477–486, (1988).

[9] Lam, K. Y., Hung, K. C., and Chow, S. T. Vibration analysis of plates with cutouts by the modified Rayleigh-Ritz method, *Applied Acoustics*, **28**(1), 49–60, (1989).

[10] Lam, K. Y. and Hung, K. C. Orthogonal polynomials and subsectioning method for vibration of plates, *Computers and Structures*, **34**(6), 827–834, (1990).

[11] Lee, H. P., Lim, S. P., and Chow, S. T. Prediction of natural frequencies of rectangular plates with rectangular cutouts, *Computers and Structures*, **36**, 861–869, (1990).

[12] Mundkar, G., Bhat, R. B., and Neriya, S. Vibration of plates with cutouts using boundary characteristics orthogonal polynomial functions in the Raleigh-Ritz method, *Journal of Sound and Vibration*, **176**(1), 136–144, (1994).

[13] Burgemeister, K. A. and Hansen, C. H. Calculating resonance frequencies of perforated panels, *Journal of sound and vibration*, **196**(4), 387–399, (1994).

[14] Young, P. G., Yuan, J., and Dickinson, S. M. Three dimensional analysis of the free vibration of thick rectangular plates with depressions, grooves or cutouts, *American Society of Mechanical Engineers Journal of Vibration and Acoustics*, **118**(2), 184–189, (1996).

[15] Sivasubramonian, B., Kulkarni, A. M., and Rao, G. V. Free vibration of curved panels with cutouts, *Journal of Sound and Vibration*, **200**(2), 227–234, (1997).

[16] Sivasubramonian. B., Rao, G. V., and Krishnan, A. Free vibration of longitudinally stiffened curved panels with cutouts, *Journal of Sound and Vibration*, **226**(1), 41–55, (1999).

[17] Grossi, R. O., Del V. Arenas, B., and Laura, P. A. A. Free vibration of rectangular plates with circular openings, *Ocean Engineering*, **24**(1), 19–24, (1997).

[18] Suhn, C., Kyeonghoon, J., Taewan, K., Soo, K. K., Bae, P. K. Free vibration analysis of perforated plates using equivalent elastic properties, *Journal of the Korean Nuclear Society*, **30**(4), 416–423, (1998).

[19] Huang, M., and Sakiyama, T. Free vibration analysis of rectangular plates with variously shaped holes, *Journal of Sound and Vibration*, **226**(4), 769–786, (1999).

20 Sahu, S. K. and Datta, P. K. Dynamic stability of curved panels with cutouts, *Journal of Sound and Vibration*, **251**(4), 683–696, (2003).

21 Avalos, D. R. and Laura, P. A. A. Transverse vibrations of simply supported rectangular plates with two rectangular cut outs, *Journal of Sound and Vibration*, **267**(4), 967–977, (2003).

22 Liew, K. M., Kitipornchai, S., Leung, A. Y. T., and Lim, C.W. Analysis of the free vibration of rectangular plates with central cut-outs using the discrete Ritz method, *International Journal of Mechanical Sciences*, **45**(5), 941–959, (2003).

23 Wang, W. C., and Lai, K. H. Hybrid determination of equivalent characteristics of perforated plates, *Experimental Mechanics*, **43**(2), 163–172, (2003).

24 Sinha, J. K., Singh, S., and Rao, A. R. Added mass and damping of submerged perforated plates, *Journal of Sound and Vibration*, **260**(3), 549–564, (2003).

25 Wu, D., Peddieson, J., Buchanan, G. R., and Rochelle, S. G. Large axisymmetric deformations of elastic/plastic perforated circular plates, *Journal of Pressure Vessel Technology*, **125**(4), 357–364, (2003).

26 Bhattacharya, A., and Raj, V. V. Peak stress multipliers for thin perforated plates with square arrays of circular holes, *International Journal of Pressure Vessels and Piping*, **80**(6), 379–388, (2003).

27 Britan, A., Karpov, A. V., Vasilev, E. I., Igra, O., Ben-Dor, G., and Shapiro., E. experimental and numerical study of shock wave interaction with perforate plates, *Journal of Fluids Engineering*, **126**, 399–409, (2004).

28 Bhattacharya, A., and Raj, V. V. yield criterion for thin perforated plates with square penetration pattern, *Journal of Pressure Vessel Technology*, **126**, 169–175, (2004).

29 Pedersen, N. L. Optimization of holes in plates for control of eigenfrequencies, *Journal of Structural and Multidisciplinary Optimization*, **28**, 1–10, (2004).

30 Lee, J.-K. and Kim, J.-G. An analytical study on prediction of effective elastic constants of perforated plate, *Journal of Mechanical Science and Technology*, **19**(12), 2224–2230, (2005).

31 Azhari, M., Shahidi, A. R., and Saadatpour, M. M. Local and post local buckling of stepped and perforated thin plates, *Applied Mathematical Modelling*, **29**, 633–652, (2005).

32 Rezaeepazhand, J. and Jafari, M. Stress analysis of perforated composite plates, *Composite Structures*, **71**, 463–468, (2005).

33 Hung, M. J., and Jo, J. C. Equivalent material properties of perforated plate with triangular or square penetration pattern for dynamic analysis, *Nuclear Engineering and Technology*, **38**, 689–696, (2006).

34 Watanabe, O., and Koike, T. Creep-fatigue life evaluation method for perforated plates at elevated temperature, *Journal of Pressure Vessel Technology*, **128**(1), 17–24, (2006).

35 Jeong, K.-H., and Amabili, M. Bending vibration of perforated beams in contact with a liquid, *Journal of Sound and Vibration*, **298**(1–2), 404–419, (2006).

36 Kathagea, K., Misiekb, T. H., and Saal, H. Stiffness and critical buckling load of perforated sheeting, *Thin-Walled Structures*, **44**(12), 1223–1230, (2006).

37 Paik, J. K. Ultimate strength of perforated steel plates under edge shear loading, *Thin-Walled Structures*, **45**(3), 301–306, (2007).

38 Paik, J. K. Ultimate strength of perforated steel plates under combined biaxial compression and edge shear loads, *Thin-Walled Structures*, **46**(2), 207–213, (2008).

39 Liu, T., Wang, K., Dong, Q.-W., and Liu, M.-S. Hydro elastic natural vibrations of perforated plates with cracks, *Procedia Engineering*, **1**(1), 129–133, (2009).

40 Cheng, B. and Zhao, J. Strengthening of perforated plates under uniaxial compression: Buckling analysis, *Thin-Walled Structures*, **48**(12), 905–914, (2010).

41 Romero, G. G., Alans, E. E., Martnez, C. C., Nallim, L. G., Toledo, M. W., lvarez, L. Vibration analysis of perforated plates using time-average digital speckle pattern interferometry, *Experimental Mechanics*, **50**(7), 1013–1021, (2010).

42 Mali, K. D. and Singru, P. M. Determination of the fundamental frequency of perforated plate with rectangular perforation pattern of circular holes by negative mass approach for the perforation, *International Journal of Advanced Materials Manufacturing and Characterization*, **1**(1), 105–109, (2012).

43 Mali, K. D. and Singru, P. M. Determination of the fundamental frequency of perforated rectangular plates: Concentrated negative mass approach for the perforation, *Advances in Acoustics and Vibrations*, **2013**, 1–6, (2013).

44 Mali, K. D. and Singru, P. M. An analytical model to determine fundamental frequency of free vibration of perforated plate by using greatest integer functions to express non homogeneity, *Advanced Materials Research*, **622**, 600–604, (2012).

45 Mali, K. D. and Singru, P. M. An analytical model to determine fundamental frequency of free vibration of perforated plate by using unit step functions to express non homogeneity, *Journal of Vibroengineering*, **14**(3), 1292–1298, (2012).

46 Mali, K. D. and Singru, P. M. An analytical model to determine fundamental frequency of rectangular plate having rectangular array of circular perforations, *Journal of Vibroengineering*, **15**(2), 588–596, (2013).

47 Chakraverty, S. *Vibration of Plates*, Boca Raton, CRC Press Taylor & Francis Group, (2009), 83–135.

48 Piersol, A. G., and Paez, T. L. *Harris' Shock and Vibration Handbook*, New York, McGraw-Hill (2002), 6th ed., 440–461.

49 Larson and Davis, Inc., ViRTe3000+ Real Time Analyzer Reference Manual, New York, Larson and Davis Publication Division., (2008).

50 Leissa, Arthur W., and Mohamad S. Qatu. *Vibration of Continuous Systems*. New York, McGraw Hill,(2011), 1st ed., 229-231.